Matthew L. Johnson,[1] Klaus Distelmaier,[1] Ian R. Lanza,[1] Brian A. Irving,[1] Matthew M. Robinson,[1] Adam R. Konopka,[1] Gerald I. Shulman,[2] and K. Sreekumaran Nair[1]

Mechanism by Which Caloric Restriction Improves Insulin Sensitivity in Sedentary Obese Adults

Diabetes 2016;65:74–84 | DOI: 10.2337/db15-0675

Caloric restriction (CR) improves insulin sensitivity and reduces the incidence of diabetes in obese individuals. The underlying mechanisms whereby CR improves insulin sensitivity are not clear. We evaluated the effect of 16 weeks of CR on whole-body insulin sensitivity by pancreatic clamp before and after CR in 11 obese participants (BMI = 35 kg/m^2) compared with 9 matched control subjects (BMI = 34 kg/m^2). Compared with the control subjects, CR increased the glucose infusion rate needed to maintain euglycemia during hyperinsulinemia, indicating enhancement of peripheral insulin sensitivity. This improvement in insulin sensitivity was not accompanied by changes in skeletal muscle mitochondrial oxidative capacity or oxidant emissions, nor were there changes in skeletal muscle ceramide, diacylglycerol, or amino acid metabolite levels. However, CR lowered insulin-stimulated thioredoxin-interacting protein (TXNIP) levels and enhanced nonoxidative glucose disposal. These results support a role for TXNIP in mediating the improvement in peripheral insulin sensitivity after CR.

More than one-third of adults and 17% of youth in the U.S. are obese (1). Obesity is associated with reduced insulin sensitivity (insulin resistance), with a high predilection to develop type 2 diabetes (T2D), hypertension, hyperlipidemia, and cardiovascular disease. Obesity results from the imbalance between energy intake and energy expenditure. Altered function of skeletal muscle mitochondria (2), the predominant organelle responsible for cellular energy metabolism, is reported to occur in obese people. Moreover, increased oxidative stress (3,4) and accumulation of lipids, ceramides, and diacylglycerol (DAG) are reported to occur in insulin-resistant states, including in obesity (5–9). Altered glucose (10), fatty acid (11), and amino acid metabolism (12) are reported in obese people, including an inability to adjust to fuel availability (13,14). Together, these data support a hypothesis that the failure to safely partition a chronic fuel surplus contributes to insulin resistance. Consistent with this hypothesis, reducing caloric intake is a successful therapeutic strategy to improve insulin sensitivity (15,16).

Caloric restriction (CR) improves insulin sensitivity (17) and reduces the incidence of diabetes and related metabolic disorders. The underlying molecular and cellular mechanisms of improved insulin sensitivity in skeletal muscle, however, remain to be fully understood. An investigation of CR on muscle mitochondrial physiology reported that CR enhanced insulin sensitivity without improving mitochondrial function (18). A 16-week CR intervention was reported to decrease total skeletal muscle DAG and ceramide content (17) in obese people; however, whether these declines in lipid metabolites were related to the dietary differences before these measurements was not clear. Moreover, the changes in DAG and ceramide after CR did not correlate with improvements in insulin sensitivity, suggesting additional pathways might be involved (17).

Emerging evidence suggests a role for thioredoxin-interacting protein (TXNIP), an α-arrestin family member, as a key negative regulator of insulin-stimulated glucose uptake (19–21) and in cellular fuel substrate partitioning in

[1]Division of Endocrinology and Metabolism, Mayo Clinic College of Medicine, Rochester, MN
[2]Howard Hughes Medical Institute and the Departments of Medicine and Cellular & Molecular Physiology, Yale University School of Medicine, New Haven, CT
Corresponding author: K. Sreekumaran Nair, nair@mayo.edu.

Received 20 May 2015 and accepted 26 August 2015.
Clinical trial reg. no. NCT01497106, clinicaltrials.gov.
This article contains Supplementary Data online at http://diabetes.diabetesjournals.org/lookup/suppl/doi:10.2337/db15-0675/-/DC1.

See accompanying article, p. 16.

skeletal muscle (22). TXNIP-deficient mice, for example, exhibit hypoglycemia during prolonged fasting (20), maintain skeletal muscle insulin sensitivity when challenged with a high-fat diet (19,21), and are unable to utilize lipid fuels (22). Moreover, high levels of TXNIP in vitro decrease insulin-stimulated glucose transport (23) and elevate cellular oxidative stress (24). Furthermore, insulin-resistant individuals and those with T2D exhibit elevations in TXNIP mRNA (23). Hence TXNIP represents a potential key regulator of insulin-stimulated glucose transport in skeletal muscle and might be involved in the improvement in metabolic inflexibility and insulin sensitivity imparted by CR.

To address these knowledge gaps, we performed a pilot study in which we systematically evaluated whole-body insulin sensitivity using the pancreatic clamp technique before and after 16 weeks of CR or control (CON). The CR program was designed to reduce total body weight by ~10% without changing physical activity levels. We hypothesized that CR would improve peripheral insulin sensitivity and that the improvement could be explained by reductions in insulin-stimulated TXNIP expression. We therefore determined skeletal muscle TXNIP mRNA expression and protein content after a hyperinsulinemic-euglycemic clamp in the postabsorptive state. Other purported causes of skeletal muscle insulin resistance were also measured after an overnight fast, including mitochondrial energetics, mitochondrial (mt)H_2O_2 emissions, whole-body metabolic flexibility, skeletal muscle DAG, ceramide, amino acids, and plasma inflammatory factors to provide a more comprehensive understanding of the effects of CR on skeletal muscle insulin resistance.

RESEARCH DESIGN AND METHODS

Experimental Procedures

For the baseline studies, 29 participants gave written informed consent, which was approved by the Mayo Foundation Institutional Review Board. Participants were included if their BMI was ≥30 kg/m^2 and they were between the ages of 45 and 65 years at the time of screening. Exclusion criteria were smoking, participation in a structured exercise program more than twice weekly for ≥30 min, fasting blood glucose value ≥7 mmol/L, or taking medications known to affect energy metabolism or insulin sensitivity, renal failure (serum creatinine >1.5 mg/dL), chronic active liver disease (aspartate aminotransferase and alanine aminotransferase >3 times normal), anticoagulant therapy, or active coronary artery disease.

Before and after 16 weeks of CR or CON, two outpatient visits and one inpatient visit were scheduled. Before the outpatient visits, participants were instructed to fast overnight from 10:00 P.M. the evening before and to avoid strenuous exercise for 24 h preceding the visits. One outpatient visit consisted of an MRI to measure subcutaneous and visceral fat distribution and magnetic resonance spectroscopy to measure skeletal muscle oxidative capacity (25). The second outpatient visit was for measurements of resting energy expenditure (REE) for the calculation of a weight-maintenance diet (Parvo Medics TrueOne 2400 Canopy system), DEXA scan (Lunar DPX-L; Lunar Radiation, Madison, WI), and VO_2peak test on a bicycle ergometer (Fig. 1).

Participants were admitted to the Clinical Research Unit (CRU) on the evening of the fifth day of the weight-maintaining diet provided by the CRU metabolic kitchen (Supplementary Fig. 1). The weight-maintenance meals (diet composition: 20% protein, 30% fat, 50% carbohydrate) were monitored daily to ensure that the correct calorie level was achieved. Upon admission to the CRU, no calories were consumed after 2100 h to achieve a 10-h fast before the two-stage insulin euglycemic pancreatic clamp the following morning, as previously published (26), with modifications as follows: the following morning at 0400 h, a primed [6,6$^2H_2$]glucose bolus (6 mg · kg fat-free mass[FFM]$^{-1}$) was administered, followed by a 9-h continuous infusion of [6,6$^2H_2$]glucose (started at 4 mg · kgFFM^{-1} · h^{-1} then titrated downward over the infusion time period to match anticipated changes in endogenous glucose production [EGP]). At 0600 h, gas exchange was measured by indirect calorimetry for 30 min for REE determination. Then at 0700 h, glucagon (0.001 μg · kgFFM^{-1} · min^{-1}), somatostatin (0.093 μg · kgFFM^{-1} · min^{-1}), and growth hormone (0.0047 μg · kgFFM^{-1} · min^{-1}) were infused for 6 h. Insulin was infused from 0700 to 1000 h at 0.62 mU · kgFFM^{-1} · min^{-1} and then from 1000 to 1300 h at 2.3 mU · kgFFM^{-1} · min^{-1}. A 40% dextrose with 2% enrichment of [6,6$^2H_2$]glucose was infused as needed to maintain blood glucose above 4.7 mmol/L from 0700 to 1000 h and then between 4.7 and 5.3 mmol/L from 1000 to 1300 h.

Blood samples were collected in a heated hotbox (131°F) through a retrograde intravenous catheter at baseline for glucose and hormone levels, and every 10 min during the clamp to maintain euglycemia. In addition, blood samples were collected every 20 min from 0600 to 0700, 0900 to 1000, and 1200 to 1300 to measure plasma [6,6$^2H_2$]glucose. At 1330 h, a percutaneous needle muscle biopsy specimen (350–400 mg) was obtained from the vastus lateralis muscle under local anesthesia, immediately frozen in liquid nitrogen, and stored at −80°F for future analysis (27). This biopsy sample was used for analysis of TXNIP mRNA and protein content. The participant remained in the CRU through the remainder of the day and was given a weight-maintenance diet until 2200 h.

At 0700 h the following morning, a second muscle biopsy specimen was obtained under local anesthesia, and ~100 mg was used immediately for mitochondrial function measurements of isolated mitochondria and mtH_2O_2 emissions (28). The remainder was immediately frozen in liquid nitrogen and stored at −80°F for future analysis, including DAG, ceramide, and amino acid measurements (Fig. 1).

Study Intervention

After the baseline study visits, participants were randomly assigned to CR or CON for 16 weeks. The CR

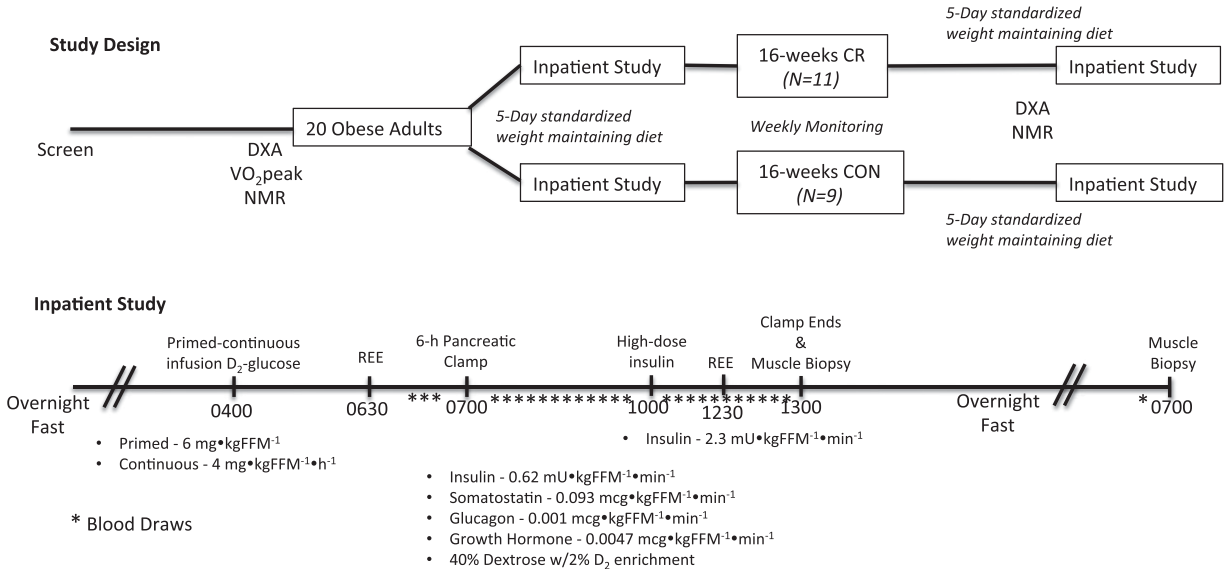

Figure 1—Experimental design. Before and after 16 weeks of CR or CON, two outpatient visits and one inpatient visit were scheduled. One outpatient visit consisted of nuclear magnetic resonance (NMR) imaging, and the second outpatient visit was for measurements of REE, DEXA scan, and a VO_2peak test on a bicycle ergometer. An inpatient visit at baseline and after 16 weeks of the intervention was conducted after 5 days of a weight-maintaining diet provided by the CRU metabolic kitchen. The inpatient visit consisted of a two-stage (low- and high-dose insulin) hyperinsulinemic-euglycemic pancreatic clamp over 6 h, followed by a skeletal muscle biopsy. Blood samples were obtained every 10 min to adjust the GIR to maintain euglycemia at ~90 mg/dL. After the clamp and biopsy were completed, standardized meals were provided to keep participants' weight stable. The following morning in the postabsorptive state, a second fasted skeletal muscle biopsy was performed. *Blood draw.

program consisted of removing 1,000 kcal from the participant's daily allowance of fat and carbohydrate. Protein content (g/day) remained constant. To assist in achieving a 1,000 kcal daily deficit, participants were provided meals from the Mayo Clinic CRU kitchen for the first 5 days and met with a registered dietitian weekly or more frequently if needed throughout the entire intervention to monitor weight loss and adherence to the CR diet. Portioned meal replacement products (New Lifestyle Diet Inc., San Ramon, CA) were also provided as needed by the dietitians throughout the intervention to assist in adherence. A participant who failed to lose weight on 2 consecutive weeks with the dietitians was provided with meals from the metabolic kitchen for another 5 days, together with additional weekly meetings to appropriately address adherence. The CON group participants were instructed to maintain their normal eating and activities of daily living. Both groups were instructed to wear an accelerometer throughout the 16-week period to ensure the daily physical activity level did not differ between groups or vary throughout the time of the intervention (data not shown).

Mitochondrial Energetics

Respiration of isolated mitochondria with glutamate and malate substrates were performed, as previously described (28), on the biopsy sample taken after an overnight fast. Briefly, mitochondria were isolated from fresh tissue by differential centrifugation. Respiration of isolated mitochondria was measured by high-resolution respirometry (Oxygraph; Oroboros Instruments, Innsbruck, Austria) using a stepwise protocol to evaluate various components of the electron transport system. Protein content of the mitochondrial suspension was measured using a colorimetric assay (Pierce 660-nm Protein Assay). Oxygen flux rates are expressed per tissue-wet weight and per milligram of mitochondrial protein.

mtH_2O_2 Emissions

The reactive oxygen species–emitting potential (mtH_2O_2) of isolated mitochondria was evaluated under state 2 conditions, as described previously (25), on the second biopsy sample taken after an overnight fast. Briefly, a Fluorolog 3 (Horiba Jobin Yvon) spectrofluorometer with temperature control and continuous stirring was used to monitor Amplex Red (Invitrogen, Carlsbad, CA) oxidation in a freshly isolated mitochondrial suspension. Amplex Red oxidation was measured in the presence of glutamate (10 mmol/L), malate (2 mmol/L), and succinate (10 mmol/L). The fluorescent signal was corrected for background auto-oxidation and calibrated to a standard curve. H_2O_2 production rates were expressed relative to mitochondrial protein.

Glucose Kinetic Calculations

Glucose concentration was measured every 10 min during the insulin clamp with an Analox glucose analyzer (Analox Instruments, London, U.K.). [6,6-$^2H_2$]-D-glucose enrichment in the plasma and infusate was measured using gas chromatography–mass spectrometry. As described

previously, the steady-state equations of Steele et al. (29) were used to calculate the rate of glucose appearance (Ra) and disappearance (Rd). EGP was calculated as the difference between total glucose Ra and the exogenous glucose infusion rate, peripheral insulin sensitivity was assessed from the rate of glucose infusion required to maintain euglycemia during the high-dose insulin clamp, and hepatic insulin sensitivity was assessed by the extent to which EGP was suppressed from baseline to low-dose hyperinsulinemia (26).

Metabolic Flexibility

The rates of energy expenditure, lipid, and carbohydrate oxidation were calculated from pulmonary gas exchange using the equations of Lusk (30), for which the rate of amino acid oxidation over the inpatient study periods was assumed to be unchanged within participants (31). Nonoxidative glucose disposal was calculated from glucose Rd in the last 30 min of the insulin clamp minus total carbohydrate oxidation.

Skeletal Muscle Amino Acid and Lipid Metabolite Measurements

All measurements were made on the second biopsy sample taken after an overnight fast. Concentrations of amino acids and metabolites were determined using MassTrak Amino Acid Solution (Waters) modified for mass spectrometry as previously described (32). Muscle samples were spiked with internal standards for amino acids and metabolites, deproteinated using cold methanol, and centrifuged. An aliquot of the supernatant was derivatized using 6-aminoquinolyl-N-hydroxysuccinimidyl carbamate and separated with an Acquity ultraperformance liquid chromatograph. Mass detection was performed using a TSQ Ultra 182 Quantum mass spectrometer (Thermo Finnigan) in electrospray ionization positive mode. Ceramide, cytosolic, and membrane DAG were measured as previously reported (33).

Quantitative PCR

Approximately 20 mg muscle was powered in liquid nitrogen, and total RNA was extracted using the RNeasy Fibrous Tissue kit (Qiagen) with DNAse treatment. RNA concentration and purity (absorbance at 260 nn–to–absorbance at 280 nn ratio >2.0 for all samples) were determined by spectrophotometry (Nanodrop), then 2 μg RNA were converted to cDNA according to the manufacturer's instructions (Applied Biosystems). Quantitative real-time PCR was performed in 384-well clear plates with 20 μL reaction volume using 20 ng cDNA. Amplification conditions were 10 min at 60°C, followed by 40 cycles of denaturing (95°C for 15 s) and annealing (60°C for 60 s) using a ViiA7 thermocycler (Applied Biosystems). Samples were amplified with multiplex conditions in triplicate on a single plate with a no template control, internal repeated control, and 7-point relative standard curve spanning 4 log dilutions. Primers and probes were commercially produced (Applied Biosystems) for TXNIP (Assay ID# Hs01006900_g1, context sequence TTATACT GAGGTGGATCCCTGCATC) and reference gene β-2-microglobulin (Assay ID# 4326319E). Efficiencies of the target and reference genes were similar (~95–100%) from the standard curve.

Western Blots

Frozen muscle tissue was pulverized in liquid nitrogen and homogenized on ice in a lysis buffer containing 100 mmol/L NaCl, 20 mmol/L Tris-HCl, 0.5 mmol/L EDTA, 0.5% (v/v) Nonidet P40, and phosphatase and protease inhibitors. Homogenates were incubated on ice for 20 min, followed by centrifugation at 10,000*g* to remove insolubilized fragments. An aliquot of the supernatant containing solubilized proteins was used for protein estimation using a detergent and reducing agent–compatible protein assay kit (Pierce 660, Thermo-Fisher Scientific, Rockford, IL). On the basis of results from the protein estimate, samples were prepared in a lithium dodecyl sulfate sample buffer (NuPAGE LDS Sample Buffer, Invitrogen) with 5% 2-mercaptoethanol to achieve a final concentration of 2 μg/μL. Samples were heated at 70°C for 10 min, and 20 μg protein was added to each well of precast gels (NuPAGE Novex Bis-Tris Mini Gels, Invitrogen). Proteins were separated by electrophoresis and blotted to polyvinylidene fluoride membranes. Membranes were then blocked with LiCor blocking buffer before incubating overnight with primary antibodies for TXNIP (Abcam ab114981) and vinculin protein (CP74, Calbiochem, EMD Millipore Corp., Billerica, MA). Proteins were detected using infrared fluorescent detection (LI-COR Odyssey, Lincoln, NE) using anti-mouse and rabbit secondary antibodies. Signal intensity was determined using LI-COR 3.0.3 imaging software.

Statistical Analyses

Statistical analysis was performed using Prism 6.0e software (GraphPad Software Inc., La Jolla, CA). Differences between group (CR vs. CON) and time were compared using a repeated-measures two-way ANOVA. When a significant interaction was detected, post hoc analysis was performed with the Sidak procedure. Age and VO_2 peak at baseline were compared using an unpaired Students *t* test. For outcomes where a significant change was found due to the intervention, a Pearson correlation was performed between the change in the GIR and change in the outcome variable (i.e., ΔTXNIP). Significance was set at $P < 0.05$. Data are presented as means ± SEM.

RESULTS

Anthropometric Characteristics

Twenty-nine participants underwent randomization after enrollment into the study, with 13 assigned to CR and 16 assigned to CON. Two CR participants and 7 CON participants were lost to follow-up; therefore, 11 completed the CR and 9 completed the CON protocol. Main clinical characteristics at baseline and postintervention are reported in Table 1. Two CR participants and one

CON participant were receiving statin therapy at baseline. At baseline, both groups were similar in age, body composition, BMI, free fatty acid (FFA) concentrations, β-hydroxybutyrate concentrations, and cardiorespiratory fitness (VO_2peak). Body weight, lean mass, and fat mass were higher in the CON group at baseline. After the 16-week intervention, total body weight, visceral fat, subcutaneous fat, BMI, body fatness, and fasting insulin concentrations all decreased in the CR group, but there was no change in CON participants. Although FFA concentrations did not change, fasting β-hydroxybutyrate concentrations increased in the CR group. Participants in the CR group lost on average 10.1 ± 1.2% of total body weight during the 16-week period.

Insulin Sensitivity and Indirect Calorimetry

The integrated area under the curve (AUC) for the GIR required to maintain euglycemia during the last hour of the clamp increased from baseline to follow-up ($P < 0.05$, Fig. 2*A–C*) with the AUC for the last hour equal to 431 ± 73.7 to 629 ± 61.7 mg · $kgFFM^{-1}$ · min^{-1} in the CR group, indicating that CR increased insulin sensitivity, whereas no change was found in the CON group (600 ± 94.3 to 610 ± 104.6 mg · $kgFFM^{-1}$ · min^{-1}). This corresponded to a glucose Rd on high-dose insulin of 7 ± 1.1 to 11 ± 0.9 ($P < 0.05$) and 9 ± 1.4 to 9 ± 1.5 mg · $kgFFM^{-1}$ · min^{-1} in the CR and CON groups, respectively. Because randomization resulted in the CON group having a significantly higher AUC at baseline than the CR group and CR increased the AUC to a similar level to that of the CON group, we compared the AUC for the last hour from a reference population of nine lean but sedentary participants (66 ± 0.4 years, BMI 27 ± 1.1 kg/m^2) who underwent an identical clamp procedure and found the lean participants exhibited a significantly higher AUC of 848 ± 68.7 mg · $kgFFM^{-1}$ · min^{-1} ($P < 0.05$) compared with the CON and CR group in the current study, demonstrating that indeed both groups were insulin resistant. EGP did not change after CR (3 ± 0.3 to 3 ± 0.1 mg · $kgFFM^{-1}$ · min^{-1}) and did not change in CON (3 ± 0.8 to 3 ± 0.4 mg · $kgFFM^{-1}$ · min^{-1}), whereas the percentage suppression of EGP from fasting to low-dose insulin slightly increased but did not reach statistical significance after CR (Fig. 2*C* and *E*). No change in the percentage suppression of EGP was found in CON (Fig. 2*C* and *E*). Insulin, glucagon, and growth hormone levels were effectively clamped, and C-peptide levels were repressed throughout the 6-h clamp (Supplementary Fig. 2). Indirect calorimetry measurements after an overnight fast (basal) showed a significant decrease in the respiratory exchange ratio (RER) after CR compared with CON ($P < 0.05$). That decrease in the fasting RER drove increased lipid oxidation during basal conditions and the significant increase in ΔRER from basal to clamp conditions after CR ($P < 0.05$, Table 2). CR significantly increased nonoxidative glucose disposal under clamp conditions ($P < 0.05$, Table 2).

Table 1—Characteristics of the subjects

	CR		Control		*P*		
Characteristic	Baseline (*N* = 11)	Post (*N* = 11)	Baseline (*N* = 9)	Post (*N* = 9)	Group	Time	Interaction
Age, year	55.3 ± 1.8		52.7 ± 1.6		—	—	—
Height, cm	169.6 ± 2.4		177.8 ± 3.9				
Weight, kg	101.8 ± 4.9	91.3 ± 4.6****	109 ± 7.4	110.3 ± 7.7	0.1401	<0.001	<0.001
Weight % change		−10.1 ± 1.2		+0.8 ± 0.6	—	—	—
BMI, kg/m^2	35.2 ± 1.3	31.8 ± 1.1****	34.4 ± 1.4	34.6 ± 1.5	0.6103	<0.001	<0.001
Glucose, mg/dL	106.6 ± 2.5	102.3 ± 2.2	105.0 ± 3.3	105.3 ± 4.1	0.8716	0.1161	0.0767
Insulin, μIU/mL	12.7 ± 1.8	6.7 ± 0.9****	11.3 ± 2.5	11.2 ± 2.3	0.5616	<0.002	<0.002
FFA, mmol/L	0.38 ± 0.04	0.45 ± 0.05	0.38 ± 0.06	0.39 ± 0.03	0.5620	0.1876	0.3880
β-Hydroxybutyrate, mmol/L	0.23 ± 0.01	0.28 ± 0.01***	0.24 ± 0.01	0.25 ± 0.01	0.3826	0.0012	0.0387
Body fat, %	45.9 ± 1.6	42.4 ± 1.5****	43.9 ± 2.0	44.3 ± 1.8	0.9918	<0.001	<0.001
Lean mass, kg	52.5 ± 3.2	50.3 ± 2.9**	59.5 ± 5.3	59.1 ± 5.0	0.1854	0.0034	0.0347
Fat mass, kg	39.6 ± 4.6	36.8 ± 2.2****	45.9 ± 3.2	46.2 ± 3.2	0.1246	<0.001	<0.001
Visceral fat, cm^2	14.6 ± 2.2	11.4 ± 1.3*	12.1 ± 1.6	13.9 ± 1.9	0.9891	0.4132	0.0081
Subcutaneous fat, cm^2	45.1 ± 2.6	36.9 ± 2.6****	43.2 ± 3.9	44.2 ± 4.1	0.5722	0.0078	0.0015
REE, kcal/day	1,668 ± 93	1,615 ± 92	1,865 ± 128	1,867 ± 109	0.1356	0.4925	0.4745
VO_2peak, L/min	1.9 ± 0.1		2.2 ± 0.2		—	—	—

Measurements were made before randomization (baseline) and again after 16 weeks of CR or CON in the fasting state. Means ± SEM are given, and a two-way (group, time) repeated-measures ANOVA was used to compare outcomes across groups. Precise *P* values are given for the ANOVA. When a significant interaction was found, a Sidak post hoc test was performed. *$P < 0.05$; **$P < 0.01$; ***$P < 0.001$; ****$P < 0.0001$.

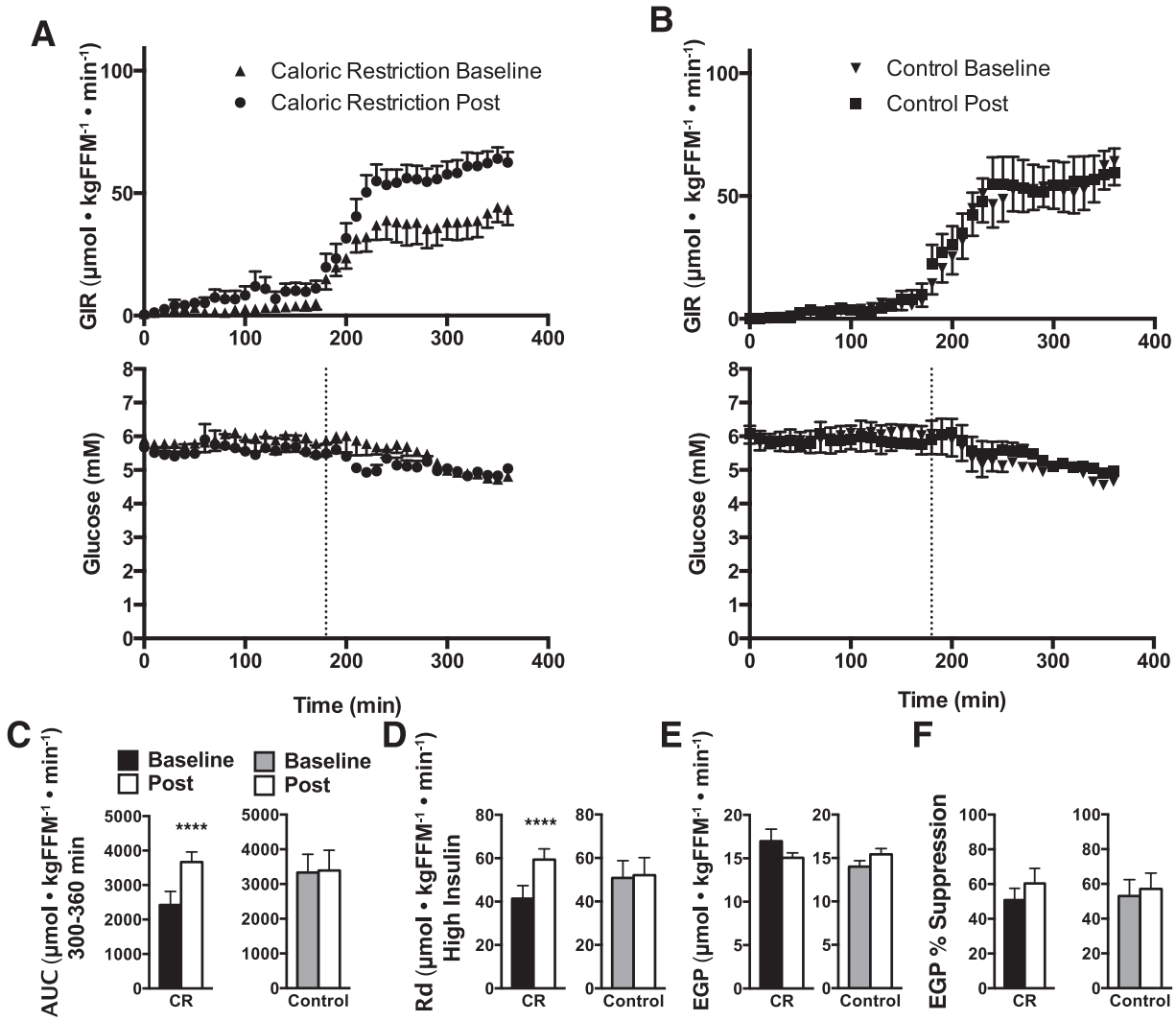

Figure 2—Insulin sensitivity. The GIR required to maintain euglycemia in 10-min intervals during the 6-h insulin infusion in CR (*A*) and CON (*B*) and corresponding glucose concentrations. *C* and *D*: The AUC and glucose Rd during the last hour of the insulin clamp for CR and CON. *E*: EGP measured in the basal fasting state. *F*: EGP percentage suppression from overnight fasted to low-dose insulin. Means ± SEM are given, and a two-way (group, time) repeated-measures ANOVA was used to compare outcomes across groups. Precise *P* values are given for the ANOVA. When a significant interaction was found, a Sidak post hoc test was performed. ****$P < 0.0001$.

Skeletal Muscle Mitochondrial Function

Ex vivo mitochondrial function did not change in either group before and after the intervention. State 3 respiration was unchanged from baseline in either group, whether expressed per tissue weight or when normalized to mitochondrial protein (Fig. 3*A–D*). These results were evident under experimental conditions where substrates were provided through respiratory chain complex I (CI, glutamate + malate), complex I and II together (CI + II, glutamate + malate + succinate), and complex II (CII, succinate + rotenone). The absence of any change in mitochondrial capacity was confirmed in vivo using nuclear magnetic resonance spectroscopy (Fig. 3*E*). In addition, there was no change in mitochondrial efficiency (i.e., decreased proton leak), evident from the respiratory control ratio (state 3/state 4), or mtH_2O_2 emissions under state 2 conditions (Fig. 3*E–G*). Together, these results demonstrate that 16 weeks of CR in obese individuals maintains but does not enhance mitochondrial function.

Lipid Metabolite Levels

Skeletal muscle analysis of total skeletal muscle ceramide, cytosolic DAG, and membrane DAG species showed no changes. In addition, no changes were found in skeletal muscle amino acid concentrations (Supplementary Figs. 3 and 4 and Supplementary Table 1).

Plasma Inflammatory Markers

Circulating CRP, interleukin-6, and tumor necrosis factor-α levels were measured after an overnight fast and found to not change in CR or CON during the intervention (Supplementary Fig. 5).

Table 2—Metabolic flexibility

	Caloric restriction		Control		*P*		
	Baseline	Post	Baseline	Post	Group	Time	Interaction
RER							
Basal	0.864 ± 0.006	0.827 ± 0.015*	0.833 ± 0.005	0.850 ± 0.012	0.7513	0.2756	0.0095
Clamp	0.917 ± 0.013	0.933 ± 0.022	0.918 ± 0.02	0.921 ± 0.022	0.6537	0.7104	0.9356
Δ	0.053 ± 0.016	0.106 ± 0.025*	0.084 ± 0.019	0.071 ± 0.028	0.9597	0.1194	0.0147
CHO oxidation (μmol · kgFFM^{-1} · min^{-1})							
Basal	16.8 ± 1.3	13.9 ± 2.2	13.3 ± 0.8	15.1 ± 1.3	0.5165	0.7066	0.0704
Clamp	21.9 ± 1.5	22.3 ± 2.8	22.1 ± 2.5	22.2 ± 2.6	0.9849	0.8653	0.9051
Nonoxidative glucose disposal (μmol · kgFFM^{-1} · min^{-1})							
Basal	0.1 ± 1.4	0.9 ± 2.2	4.9 ± 4.4	2.5 ± 2.5	0.2949	0.7894	0.5297
Clamp	15.3 ± 6.3	31.5 ± 4.9**	28.2 ± 5.9	28.9 ± 6.0	0.5141	0.0097	0.0157
Lipid oxidation (μmol · kgFFM^{-1} · min^{-1})							
Basal	1.2 ± 0.1	1.5 ± 0.1*	1.5 ± 0.1	1.4 ± 0.1	0.4743	0.3587	0.0083
Clamp	0.8 ± 0.2	0.7 ± 0.2	0.7 ± 0.1	0.7 ± 0.2	0.7956	0.4845	0.6494

Measurements were made before randomization (baseline) and again after 16 weeks of CR or CON. Means ± SEM are given, and a two-way (group, time) repeated-measures ANOVA was used to compare outcomes across groups. Precise *P* values are given for the ANOVA. When a significant interaction was found, a Sidak post hoc test was performed. CHO, carbohydrate. *$P < 0.05$; **$P < 0.01$.

TXNIP Expression Levels

TXNIP mRNA levels were measured in the vastus lateralis biopsy sample taken after the 6-h hyperinsulinemic-euglycemic clamp and the morning after an overnight 10-h fast. In the biopsy sample taken after the insulin clamp, levels of TXNIP significantly declined after the 16-week intervention in the CR group ($P < 0.05$, Fig. 4*A*). Furthermore, the change in TXNIP expression across all CR and CON participants significantly correlated with the change in GIR during the hyperinsulinemic-euglycemic clamp ($r = -0.71$, $R^2 = 0.50$, $P = 0.001$; Fig. 4*B*). We further measured TXNIP protein content in the biopsy sample after the insulin clamp to see whether the change in mRNA expression levels resulted in changes in protein content. TXNIP significantly declined after the 16-week intervention in the CR group ($P < 0.05$, Fig. 4*C*), and the change in TXNIP protein content significantly correlated with the change in GIR during the hyperinsulinemic-euglycemic clamp ($r = -0.5017$, $R^2 = 0.25$, $P = 0.034$; Fig. 4*D*). There was no change in TXNIP mRNA expression levels in the overnight fasted sample (Supplementary Fig. 6).

DISCUSSION

The finding in the current study that insulin-induced skeletal muscle TXNIP mRNA and protein expression change after CR provides novel insight into the mechanism by which peripheral insulin sensitivity is enhanced by CR in adults at high risk of developing T2D. Importantly, these findings potentially provide an important link between skeletal muscle substrate metabolism and insulin sensitivity. A primary defect in individuals with T2D is reduced skeletal muscle nonoxidative glucose disposal under insulin-stimulated conditions (34). In the current study, enhanced nonoxidative glucose disposal, likely occurring in skeletal muscle as glycogen synthesis (35), primarily accounted for higher glucose Rd (Table 2). However, we did not observe any changes in many commonly purported determinants of insulin resistance in skeletal muscle. We did not observe any effect of CR on intramuscular DAG, ceramide, or amino acid metabolites (Supplementary Figs. 3 and 4 and Supplementary Table 1). No effect on skeletal muscle mitochondrial oxidative capacity or mtH_2O_2 emissions was observed (Fig. 2). The most important finding is the significant decrease in skeletal muscle TXNIP transcript and protein expression after the hyperinsulinemic-euglycemic clamp (Fig. 4*A*) and lack of a similar change in TXNIP after the CON period. We further observed that the change in glucose Rd during the hyperinsulinemic-euglycemic clamp during the 16-week period in all participants was significantly correlated to the change in TXNIP in response to insulin (Fig. 4*B* and *D*), supporting a hypothesis that the reduction in TXNIP at least partly explains the increase in insulin-induced glucose disposal.

The results thus provide new mechanistic insight on how CR enhances insulin-stimulated glucose disposal through a key redox-sensitizing protein in skeletal muscle. TXNIP impairs insulin signaling by inhibiting thioredoxin NADPH–dependent reduction of protein disulfides on phosphatidylinositol 3-phosphatase (36). When stabilized, phosphatidylinositol 3-phosphatase has been shown to oppose insulin signaling in skeletal muscle (19,37). Furthermore, skeletal muscle TXNIP deletion that protects against high-fat diet–induced insulin resistance (19,21) is independent of any apparent changes in mitochondrial function (22). Participants in the current study showed no changes in any of the measured indices of mitochondrial function or mtH_2O_2 emissions (Fig. 3), but demonstrated changes in insulin sensitivity (Fig. 2),

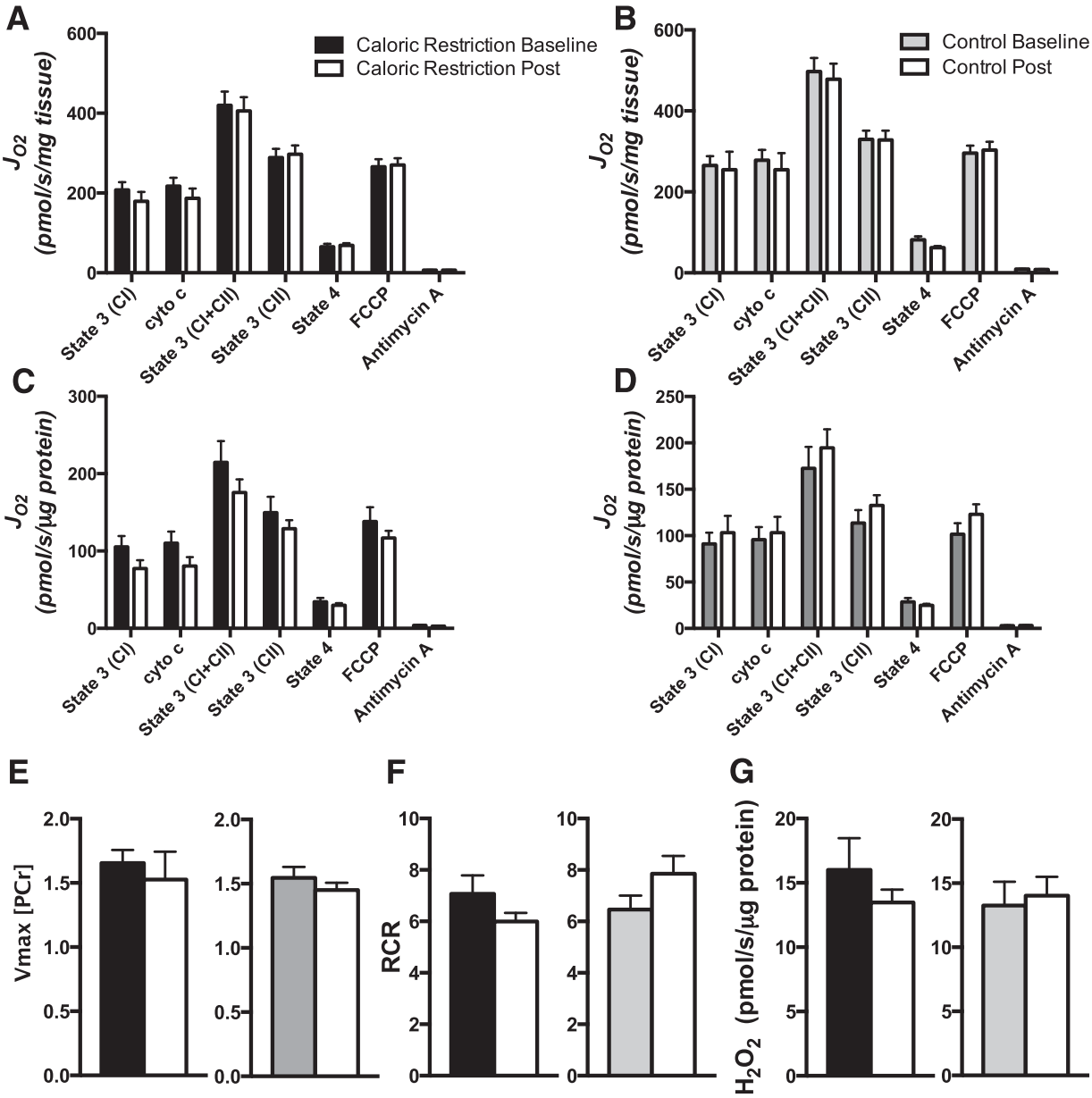

Figure 3—Mitochondrial function. Mitochondrial oxygen consumption rates (J_{O2}) were measured with carbohydrate-based mitochondrial substrates for CR (*A*) and CON (*B*) and then normalized for mitochondrial protein (*C* and *D*). *E*: In vivo oxidative capacity measured by magnetic resonance spectroscopy before and after the 16-week period. *F*: Mitochondrial coupling was assessed from the respiratory control ratio (RCR). *G*: mtH_2O_2 emissions were evaluated in isolated mitochondria under state 2 conditions. Means ± SEM are given, and a two-way (group, time) repeated-measures ANOVA was used to compare outcomes across groups.

supporting an independent role for TXNIP from mitochondrial function.

There is growing interest in understanding how lifestyle interventions such as CR mediate their insulin-sensitizing effects in obese individuals at high risk of developing T2D. We previously showed that lifelong CR enhanced skeletal muscle antioxidant status and reduced oxidative damage to proteins, suggesting improved cellular redox status (38). More recently, we demonstrated that 12 weeks of aerobic exercise training in insulin-resistant women with polycystic ovary syndrome improved insulin sensitivity, enhanced skeletal muscle endogenous antioxidant activity, reduced markers of cellular oxidative stress, and lowered chronically elevated mtH_2O_2 emissions to those of healthy control subjects. The current study demonstrated that improvement of insulin sensitivity by weight loss in CR is mediated by mechanisms other than by altered mitochondrial function, although we did not measure mitochondrial fatty acid oxidative capacity.

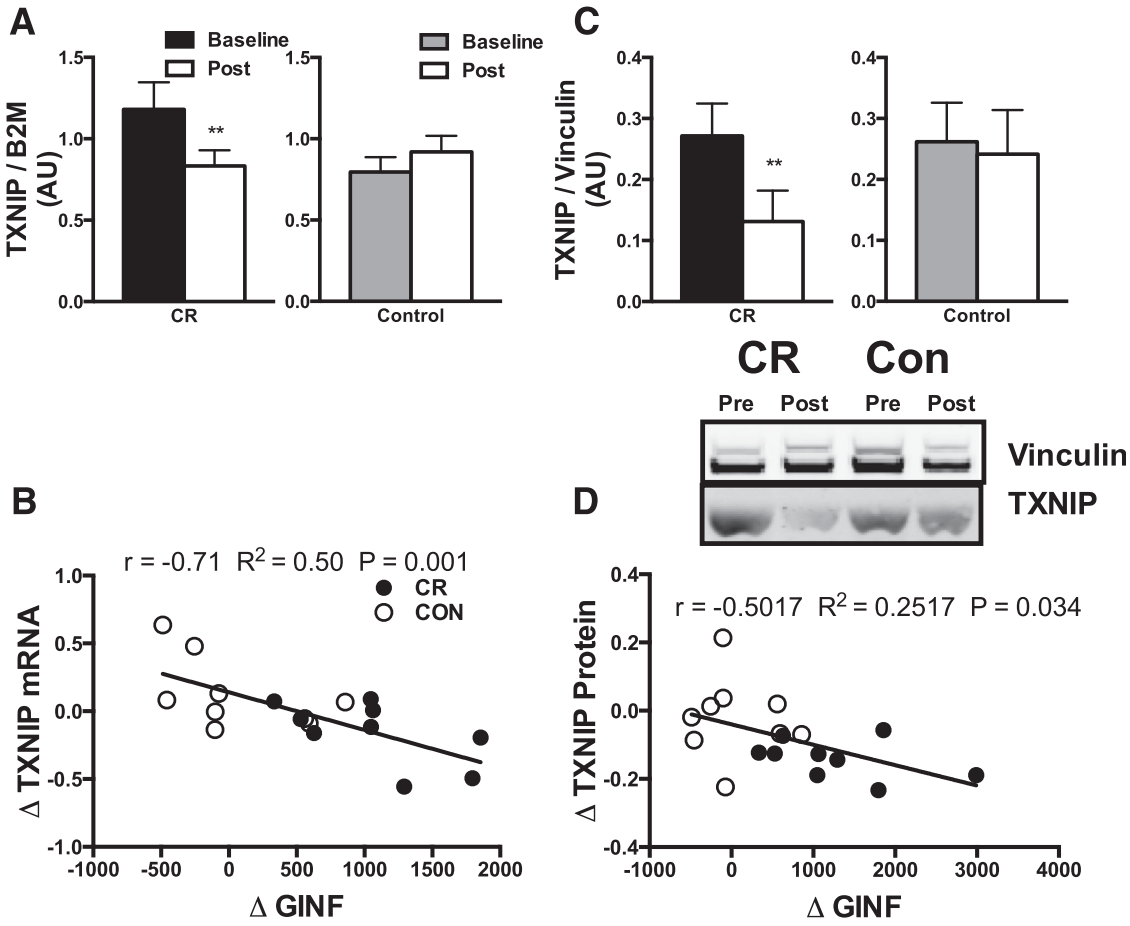

Figure 4—*A*: Skeletal muscle TXNIP expression was evaluated using quantitative PCR and normalized to β-2-microglobulin (B2M) in muscle biopsy samples after the insulin clamp. *B*: The ΔTXNIP mRNA was correlated using a Pearson correlation to the ΔAUC for the 6-h insulin clamp for all participants. *C*: Skeletal muscle protein content was evaluated using Western blot and normalized to vinculin. *D*: The ΔTXNIP protein was correlated using a Pearson correlation to the ΔAUC for the 6-h insulin clamp for all participants. ΔGINF, change in GIR. Means ± SEM are given, and a two-way (group, time) repeated-measures ANOVA was used to compare outcomes across groups. When a significant interaction was found, a Sidak post hoc test was performed. $^{**}P < 0.01$.

Early reports indicated that CR enhanced peripheral insulin sensitivity in obese individuals and in individuals with T2D in association with declines in skeletal muscle lipid content (39). However, subsequent investigations of exercise training (40,41) and acute lipid infusions in rodents (42) have identified that lipid content, although predictive of T2D risk (7,35), is unlikely to be directly involved in reducing insulin action on skeletal muscle. Instead, much work in the field has identified bioactive lipid species, including ceramide (43), DAGs (33), and elevated amino acid metabolites (44), as causes of skeletal muscle insulin resistance. We measured each of those known causes in the current study and found that CR did not change their levels in skeletal muscle but did improve peripheral insulin sensitivity. Our current results are therefore in contrast to others (17), who found significant decreases in skeletal muscle DAG and ceramide levels after 16 weeks of CR. We analyzed not only total ceramide and DAG but also the subcellular localization of DAG species that are likely to affect insulin sensitivity (Supplementary Figs. 3 and 4). Of interest, anserine, an amino acid metabolite involved in scavenging endogenous carbonyls (45), increased after CR. This may potentially contribute to the reduction of carbonylated proteins, nucleic acids, and aminophospholipids, with a potential effect on protein function. It is reasonable to state that while on CR, insulin sensitivity and many metabolites may both change, but after CR and then a weight-maintaining diet, only insulin sensitivity improves without much change in metabolites, supporting a notion that improvement of insulin sensitivity after CR-related weight loss has a mechanism unrelated to the changes in metabolites.

Insulin resistance has also been linked to metabolic inflexibility originally described across the leg in insulin-resistant individuals (13). Recent exercise training (46–48) and programs of diet plus exercise training (49) have shown improvements in metabolic inflexibility and changes in the lipid content of hepatic and skeletal muscle and insulin sensitivity. The link between metabolic inflexibility and insulin sensitivity is proposed to be through

mitochondria (50); however, metabolic inflexibility improved (Table 2) in the current study, with no changes in any indices of mitochondrial function. The improvement in metabolic inflexibility was due to higher whole-body lipid oxidation in the overnight fasted state (Table 2), a finding that is supported by elevated β-hydroxybutyrate concentrations after CR in the fasted state (Table 1). Lack of change in plasma FFA concentrations after an overnight fast on CR is consistent with a previous CR study in obese people (12) and may represent increased clearance of FFA despite increased mobilization. How metabolic flexibility, substrate partitioning, and insulin sensitivity are mechanistically linked remains to be resolved. The current study did, however, demonstrate that CR enhances insulin-stimulated glucose disposal during hyperinsulinemic conditions mainly by nonoxidative glucose disposal in the peripheral tissues that is likely to occur primarily in skeletal muscle (51).

Our two-stage pancreatic clamp technique also allowed us to evaluate the responsiveness of EGP to insulin (Fig. 2). In those with obesity and overt T2D, CR restores elevated levels of EGP to those of normal control subjects in concert with substantial declines in hepatic lipid content (52). The current results in obese individuals, who are not overt patients with diabetes, demonstrated that the effect of CR was primarily on peripheral glucose disposal, with a minimal effect on EGP, and future investigations should be focused on whether hepatic lipid content is affected by CR in insulin-resistant individuals with prediabetes.

In summary, 16 weeks of CR and related weight loss in obese participants at a high risk of developing T2D improved whole-body insulin sensitivity, with the main effect on peripheral glucose disposal. This improvement cannot be attributed to alterations in skeletal muscle mitochondrial oxidative capacity, mtH_2O_2 emissions, or intramuscular content of ceramide, DAG, or amino acid metabolites. However, the CR-induced improvement in insulin sensitivity occurred in concert with increased postabsorptive whole-body lipid oxidation. Moreover, we found that CR reduced levels of skeletal muscle TXNIP expression after hyperinsulinemia. Furthermore, the changes in TXNIP expression correlated with changes in the glucose Rd during the hyperinsulinemic state during the 16-week period. Together, these results support a likely role of TXNIP in CR-induced improvement in insulin sensitivity.

Acknowledgments. The authors are greatly indebted to the skillful assistance of Katherine Klaus, Daniel Jakaitis, Jill Schimke, Dawn Morse, Roberta Soderberg, Deborah Sheldon, Lynne Johnson, and Melissa Aakre in the Division of Endocrinology and Metabolism, Mayo Clinic College of Medicine, Rochester, MN.

Funding. Funding for this work was provided by National Institute of Diabetes and Digestive and Kidney Diseases grants U24-DK-100469, DK-50456, T32-DK-007198 (M.L.J.), T32-DK-007352 (M.M.R. and A.R.K.), R01-DK-49230 (G.I.S.), R24-DK-090963 (G.I.S.), R01-DK-41973 (K.S.N.), and UL1-TR-000135, and by National Center for Advancing Translational Sciences grants KL2-TR-000136-07 (M.L.J.) and KL2-RR-024151 (B.A.I.). Additional support was provided by the Mayo Foundation and the Murdock-Dole Professorship (to K.S.N.). Meal replacements for the caloric restriction group were donated by New Lifestyle Diet (San Ramon, CA).

Duality of Interest. No potential conflicts of interest relevant to this article were reported.

Author Contributions. M.L.J. contributed to conceptual design, data collection, analysis, and interpretation, and wrote the manuscript. K.D. contributed to data collection, data analysis, and manuscript writing and editing. I.R.L. contributed to conceptual design, data collection, data interpretation, and manuscript writing and editing. B.A.I. contributed to conceptual design, data collection, data interpretation, and manuscript writing and editing. M.M.R. and A.R.K. contributed to data collection, data analysis, and manuscript editing. G.I.S. performed tissue DAG and ceramide analyses and manuscript writing and editing. K.S.N. contributed to conceptual design, supervised the execution of the study, data analysis, data interpretation, and manuscript writing and editing. K.S.N. is the guarantor of this work and, as such, had full access to all the data in the study and takes responsibility for the integrity of the data and the accuracy of the data analysis.

Prior Presentation. Parts of this study were presented as a poster at the 75th Scientific Sessions of the American Diabetes Association, Boston, MA, 5–9 June 2015.

References

1. Ogden CL, Carroll MD, Kit BK, Flegal KM. Prevalence of childhood and adult obesity in the United States, 2011-2012. JAMA 2014;311:806–814

2. Kelley DE, He J, Menshikova EV, Ritov VB. Dysfunction of mitochondria in human skeletal muscle in type 2 diabetes. Diabetes 2002;51:2944–2950

3. Anderson EJ, Lustig ME, Boyle KE, et al. Mitochondrial H2O2 emission and cellular redox state link excess fat intake to insulin resistance in both rodents and humans. J Clin Invest 2009;119:573–581

4. Konopka AR, Asante A, Lanza IR, et al. Defects in mitochondrial efficiency and H2O2 emissions in obese women are restored to a lean phenotype with aerobic exercise training. Diabetes 2015;64:2104–2115

5. Goodpaster BH, Thaete FL, Simoneau JA, Kelley DE. Subcutaneous abdominal fat and thigh muscle composition predict insulin sensitivity independently of visceral fat. Diabetes 1997;46:1579–1585

6. Pan DA, Lillioja S, Kriketos AD, et al. Skeletal muscle triglyceride levels are inversely related to insulin action. Diabetes 1997;46:983–988

7. Krssak M, Falk Petersen K, Dresner A, et al. Intramyocellular lipid concentrations are correlated with insulin sensitivity in humans: a ^{1}H NMR spectroscopy study. Diabetologia 1999;42:113–116

8. Mayerson AB, Hundal RS, Dufour S, et al. The effects of rosiglitazone on insulin sensitivity, lipolysis, and hepatic and skeletal muscle triglyceride content in patients with type 2 diabetes. Diabetes 2002;51:797–802

9. Bergman BC, Hunerdosse DM, Kerege A, Playdon MC, Perreault L. Localisation and composition of skeletal muscle diacylglycerol predicts insulin resistance in humans. Diabetologia 2012;55:1140–1150

10. Butler PC, Rizza RA. Contribution to postprandial hyperglycemia and effect on initial splanchnic glucose clearance of hepatic glucose cycling in glucose-intolerant or NIDDM patients. Diabetes 1991;40:73–81

11. Guo Z, Hensrud DD, Johnson CM, Jensen MD. Regional postprandial fatty acid metabolism in different obesity phenotypes. Diabetes 1999;48:1586–1592

12. Henderson GC, Nadeau D, Horton ES, Nair KS. Effects of adiposity and 30 days of caloric restriction upon protein metabolism in moderately vs. severely obese women. Obesity (Silver Spring) 20109;18:1135–1142

13. Kelley DE, Goodpaster B, Wing RR, Simoneau JA. Skeletal muscle fatty acid metabolism in association with insulin resistance, obesity, and weight loss. Am J Physiol 1999;277:E1130–E1141

14. Kelley DE, Mandarino LJ. Hyperglycemia normalizes insulin-stimulated skeletal muscle glucose oxidation and storage in noninsulin-dependent diabetes mellitus. J Clin Invest 1990;86:1999–2007

15. Tuomilehto J, Lindström J, Eriksson JG, et al.; Finnish Diabetes Prevention Study Group. Prevention of type 2 diabetes mellitus by changes in lifestyle among subjects with impaired glucose tolerance. N Engl J Med 2001;344:1343–1350
16. Knowler WC, Barrett-Connor E, Fowler SE, et al.; Diabetes Prevention Program Research Group. Reduction in the incidence of type 2 diabetes with lifestyle intervention or metformin. N Engl J Med 2002;346:393–403
17. Dubé JJ, Amati F, Toledo FG, et al. Effects of weight loss and exercise on insulin resistance, and intramyocellular triacylglycerol, diacylglycerol and ceramide. Diabetologia 2011;54:1147–1156
18. Toledo FG, Menshikova EV, Azuma K, et al. Mitochondrial capacity in skeletal muscle is not stimulated by weight loss despite increases in insulin action and decreases in intramyocellular lipid content. Diabetes 2008;57:987–994
19. Hui ST, Andres AM, Miller AK, et al. Txnip balances metabolic and growth signaling via PTEN disulfide reduction. Proc Natl Acad Sci U S A 2008;105:3921–3926
20. Yoshihara E, Fujimoto S, Inagaki N, et al. Disruption of TBP-2 ameliorates insulin sensitivity and secretion without affecting obesity. Nat Commun 2010;1:127
21. Chutkow WA, Birkenfeld AL, Brown JD, et al. Deletion of the alpha-arrestin protein Txnip in mice promotes adiposity and adipogenesis while preserving insulin sensitivity. Diabetes 2010;59:1424–1434
22. DeBalsi KL, Wong KE, Koves TR, et al. Targeted metabolomics connects thioredoxin-interacting protein (TXNIP) to mitochondrial fuel selection and regulation of specific oxidoreductase enzymes in skeletal muscle. J Biol Chem 2014;289:8106–8120
23. Parikh H, Carlsson E, Chutkow WA, et al. TXNIP regulates peripheral glucose metabolism in humans. PLoS Med 2007;4:e158
24. Schulze PC, Yoshioka J, Takahashi T, He Z, King GL, Lee RT. Hyperglycemia promotes oxidative stress through inhibition of thioredoxin function by thioredoxin-interacting protein. J Biol Chem 2004;279:30369–30374
25. Lanza IR, Bhagra S, Nair KS, Port JD. Measurement of human skeletal muscle oxidative capacity by ^{31}P-MR spectroscopy: a cross-validation with in vitro measurements. J Magn Reson Imaging 2011;34:1143–1150
26. Lanza IR, Short DK, Short KR, et al. Endurance exercise as a countermeasure for aging. Diabetes 2008;57:2933–2942
27. Nair KS, Halliday D, Griggs RC. Leucine incorporation into mixed skeletal muscle protein in humans. Am J Physiol 1988;254:E208–E213
28. Lanza IR, Nair KS. Functional assessment of isolated mitochondria in vitro. Methods Enzymol 2009;457:349–372
29. Steele R, Wall JS, De Bodo RC, Altszuler N. Measurement of size and turnover rate of body glucose pool by the isotope dilution method. Am J Physiol 1956;187:15–24
30. Lusk G. Animal calorimetry twenty-fourth paper. Analysis of the oxidation of mixtures of carbohydrate and fat. J Biol Chem 1924;59:41–42
31. Robinson MM, Soop M, Sohn TS, et al. High insulin combined with essential amino acids stimulates skeletal muscle mitochondrial protein synthesis while decreasing insulin sensitivity in healthy humans. J Clin Endocrinol Metab 2014;99:E2574–E2583
32. Lanza IR, Zhang S, Ward LE, Karakelides H, Raftery D, Nair KS. Quantitative metabolomics by H-NMR and LC-MS/MS confirms altered metabolic pathways in diabetes. PLoS One 2010;5:e10538
33. Szendroedi J, Yoshimura T, Phielix E, et al. Role of diacylglycerol activation of PKCθ in lipid-induced muscle insulin resistance in humans. Proc Natl Acad Sci U S A 2014;111:9597–9602
34. Shulman GI, Rothman DL, Jue T, Stein P, DeFronzo RA, Shulman RG. Quantitation of muscle glycogen synthesis in normal subjects and subjects with non-insulin-dependent diabetes by ^{13}C nuclear magnetic resonance spectroscopy. N Engl J Med 1990;322:223–228
35. Cline GW, Petersen KF, Krssak M, et al. Impaired glucose transport as a cause of decreased insulin-stimulated muscle glycogen synthesis in type 2 diabetes. N Engl J Med 1999;341:240–246
36. Kwon J, Lee SR, Yang KS, et al. Reversible oxidation and inactivation of the tumor suppressor PTEN in cells stimulated with peptide growth factors. Proc Natl Acad Sci U S A 2004;101:16419–16424
37. Pelicano H, Xu RH, Du M, et al. Mitochondrial respiration defects in cancer cells cause activation of Akt survival pathway through a redox-mediated mechanism. J Cell Biol 2006;175:913–923
38. Lanza IR, Zabielski P, Klaus KA, et al. Chronic caloric restriction preserves mitochondrial function in senescence without increasing mitochondrial biogenesis. Cell Metab 2012;16:777–788
39. Goodpaster BH, Theriault R, Watkins SC, Kelley DE. Intramuscular lipid content is increased in obesity and decreased by weight loss. Metabolism 2000;49:467–472
40. Dubé JJ, Amati F, Stefanovic-Racic M, Toledo FGS, Sauers SE, Goodpaster BH. Exercise-induced alterations in intramyocellular lipids and insulin resistance: the athlete's paradox revisited. Am J Physiol Endocrinol Metab 2008;294:E882–E888
41. Goodpaster BH, He J, Watkins S, Kelley DE. Skeletal muscle lipid content and insulin resistance: evidence for a paradox in endurance-trained athletes. J Clin Endocrinol Metab 2001;86:5755–5761
42. Yu C, Chen Y, Cline GW, et al. Mechanism by which fatty acids inhibit insulin activation of insulin receptor substrate-1 (IRS-1)-associated phosphatidylinositol 3-kinase activity in muscle. J Biol Chem 2002;277:50230–50236
43. Chavez JA, Holland WL, Bär J, Sandhoff K, Summers SA. Acid ceramidase overexpression prevents the inhibitory effects of saturated fatty acids on insulin signaling. J Biol Chem 2005;280:20148–20153
44. Newgard CB, An J, Bain JR, et al. A branched-chain amino acid-related metabolic signature that differentiates obese and lean humans and contributes to insulin resistance. Cell Metab 2009;9:311–326
45. Aldini G, Facino RM, Beretta G, Carini M. Carnosine and related dipeptides as quenchers of reactive carbonyl species: from structural studies to therapeutic perspectives. Biofactors 2005;24:77–87
46. Meex RC, Schrauwen-Hinderling VB, Moonen-Kornips E, et al. Restoration of muscle mitochondrial function and metabolic flexibility in type 2 diabetes by exercise training is paralleled by increased myocellular fat storage and improved insulin sensitivity. Diabetes 2010;59:572–579
47. van der Heijden G-J, Toffolo G, Manesso E, Sauer PJJ, Sunehag AL. Aerobic exercise increases peripheral and hepatic insulin sensitivity in sedentary adolescents. J Clin Endocrinol Metab 2009;94:4292–4299
48. van der Heijden GJ, Wang ZJ, Chu ZD, et al. A 12-week aerobic exercise program reduces hepatic fat accumulation and insulin resistance in obese, Hispanic adolescents. Obesity (Silver Spring) 2010;18:384–390
49. Galgani JE, Heilbronn LK, Azuma K, et al.; Look AHEAD Adipose Research Group. Metabolic flexibility in response to glucose is not impaired in people with type 2 diabetes after controlling for glucose disposal rate. Diabetes 2008;57:841–845
50. Ritov VB, Menshikova EV, He J, Ferrell RE, Goodpaster BH, Kelley DE. Deficiency of subsarcolemmal mitochondria in obesity and type 2 diabetes. Diabetes 2005;54:8–14
51. DeFronzo RA, Gunnarsson R, Björkman O, Olsson M, Wahren J. Effects of insulin on peripheral and splanchnic glucose metabolism in noninsulin-dependent (type II) diabetes mellitus. J Clin Invest 1985;76:149–155
52. Petersen KF, Dufour S, Befroy D, Lehrke M, Hendler RE, Shulman GI. Reversal of nonalcoholic hepatic steatosis, hepatic insulin resistance, and hyperglycemia by moderate weight reduction in patients with type 2 diabetes. Diabetes 2005;54:603–608